

Neutron Contamination Detection of Medical Linear Accelerators by Thick Gas Electron Multiplier Detector in Self-Quenching Streamer Mode

Mohamad Hadi Najarzade¹, Mohamad Reza Rezaie^{2*}, Ali Negarestani², Ahmad Akhound¹

1. Department of Physics, Payame Noor University (PNU), Tehran, Iran
2. Department of Nuclear Engineering, Faculty of Sciences and Modern Technologies, Graduate University of Advanced Technology, Kerman, Iran

ARTICLE INFO

Article type:
Original Paper

Article history:

Received: Sept 06, 2022
Accepted: Mar 23, 2023

Keywords:

Particle Accelerators
Neutrons
Radiotherapy
Monte Carlo Method

ABSTRACT

Introduction: The presence of neutron contamination in medical linear accelerators poses a significant challenge in radiation therapy. Numerous studies have addressed the estimation of neutron levels, often relying on electronic equipment to extract simulation results. This study introduces an innovative neutron detection method that eliminates the need for electrical system with complex circuit.

Material and Methods: Neutron contamination arises in VARIAN linear accelerators through the interaction of energetic photons with heavier elements in the accelerator head, such as Tungsten. The primary objective of this study is to investigate neutron contamination in the VARIAN

linear accelerators using a Thick Gas Electron Multiplier (THGEM) detector in the Self-Quenching Streamer (SQS) mode through Monte Carlo simulation. The detection system designed in this study involves of two main parts. 1- Conversion material to convert neutrons to protons. 2- THGEM in SQS mode to detect protons. In this structure, the detection of protons gives an estimate of neutron contamination.

Results: The findings indicate that, in the designed detection system, a distance of 0.5 cm from the converter is an optimal location for the THGEM. When the THGEM's minimum voltage is set at 700 volts, SQS mode occurs in most THGEM holes.

Conclusion: The simple structure is one of the advantages of detection system in this research. Its cost-effectiveness, featuring fewer electrical tolerances, lightweight design, and adaptability in various sizes are additional advantages, making it a viable option for neutron contamination detection.

► Please cite this article as:

Najarzade MH, Rezaie MR, Negarestani A, Akhound A. Neutron Contamination Detection of Medical Linear Accelerators by Thick Gas Electron Multiplier Detector in Self-Quenching Streamer Mode. Iran J Med Phys 2024; 21: 130-137. 10.22038/IJMP.2023.67706.2178.

Introduction

Within medical linear accelerators (LINAC), the kinetic energy of electrons can reach levels of up to 25 MeV [1]. As electrons with heightened energy approach the metal target, they generate energetic photons. Neutron contamination may occur when these high-energy photons collide with the heavier elements present in the accelerator head. Key components of the linear accelerator head, including W, Al, Au, Fe, and Pb, are capable of producing neutrons [2-4]. Numerous studies have explored the nuclear interactions of high-energy Photo neutrons with heavy elements, particularly focusing on neutron contaminations around the high-energy range of linear accelerators [4-22]. Different calculation codes such as GEANT4 (Geometry and Tracking version 4) [8] and MCNPX (Monte Carlo N Particle-version X) [2, 9], along with diverse estimation methods like Bobble detector [10, 11], TLD (Thermoluminescent Dosimeter) [12, 13], and Nuclear methods [14, 15], have been employed in these studies. Some investigations have even compared the neutron

contamination of LINAC parts from various companies [20]. Besides computational codes, detectors have been developed to assess neutron contaminations and their impact on body organs [23-25]. Overall, all these studies show the importance of investigating neutron contamination in the medical linear accelerators. By detecting the number and energy of neutrons produced in these accelerators, the risks to the patient's body can be estimated. To date, significant research has focused on neutron detection methods. Converting neutrons to the charged ions such as protons and alpha is the most used way to detect neutrons. Therefore, the produced ions can be directly related to the neutron source. Various materials, including BF-3 (Boron trifluoride) or layers of Boron, have been explored as neutron converters [26-28]. Detection methods for these produced ions vary, with Gas Electron Multiplier detectors (GEM detectors) being one such option [29, 30]. GEM detectors have been utilized for detecting fast neutrons and measuring high-intensity neutrons [31, 32]. A more

*Corresponding Author: Tel: 09133425938; Email: mr.rezaie@kgut.ac.ir

recent and simpler iteration of GEM detectors, known as Thick Gas Electron Multiplier detectors (THGEM detectors), was introduced in 2007. THGEM detectors exhibit a straightforward design, affordable cost, and high response capability for detection, making them efficient (Figure 1 illustrates an image of the THGEM detector).

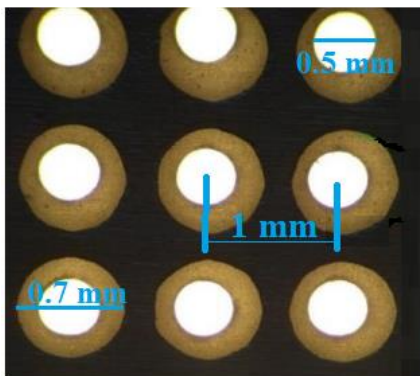


Figure 1. The THGEM detector holes

The THGEM that make in this investigation can be characterized as a flat capacitor with a thickness of 0.4mm, comprising two copper plates measuring 5×5 cm² each, separated by an FR-4 dielectric. It features 2601 holes arranged regularly in a 51×51 grid, with a hole pitch of 1 mm.

Primarily designed for detecting protons and heavy ions, the THGEM has also found application in neutron detection, including thermal neutrons. Various methods for utilizing THGEM in neutron detection exist, often requiring complex electrical circuit structures [33-34]. In this research, a novel approach to neutron detection using THGEM is proposed, wherein the holes of the detector are employed in the Self-Quenching Streamer (SQS) mode [35-37]. SQS mode operates similarly to other gas detector modes by ionizing gas atoms using an electric field. In gas detectors, uncontrolled initial ionization can lead to an ion avalanche across the detection space, causing the detector to operate in Geiger-Muller mode as a simple counter. In another case of gas detectors, the electron avalanche is controlled in a way that is proportional to primary ionization. In this case, the detector is in proportional mode [38]. Another new approach involves the use of a combination of noble gases that absorb UV photons, preventing additional avalanches and producing only a column of visible light (streamer) at the ion entry site. This mode of operation of the gas detector is called SQS mode. In this mode approach created streamer depends on initial charge density and electrical field. which aims to provide a simpler structure with fewer electrical circuits. In this method. Protons produced from the neutron-to-proton converter layer are detected when the THGEM detector is in SQS mode. The calculations for this

research are conducted using the MCNPX code, which is designed based on Monte Carlo simulation principles [39].

Materials and Methods

The process of producing and detecting contaminated neutrons

In this segment, the assessment of neutron contamination induced by the VITAL model of the VARIAN LINAC operating at 15 MeV energy is scrutinized utilizing the THGEM in SQS mode. Essential components of the linear accelerator head, including flattening filter, target and collimators are composed of materials such as Tungsten, Iron, and Copper, all possessing a threshold energy for neutron production [4,20]. Figure 2 illustrates the constituents of the Varian LINAC head through a cutaway diagram.

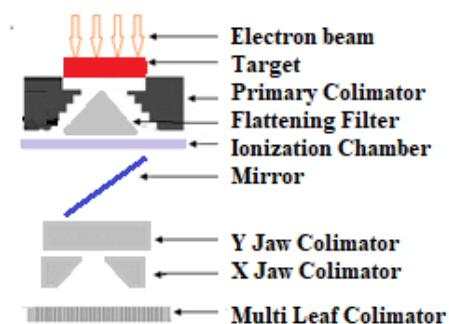


Figure 2. Diagram of VARIAN LINAC head

In this particle accelerator, energetic electrons are directed towards a metal target, generating energetic photons [3]. Photons with increased energy may collide with elements of the accelerator, giving rise to photo-neutrons (neutron contamination). Figure 3 illustrates the suggested detection system designed to estimate the presence of these neutrons.

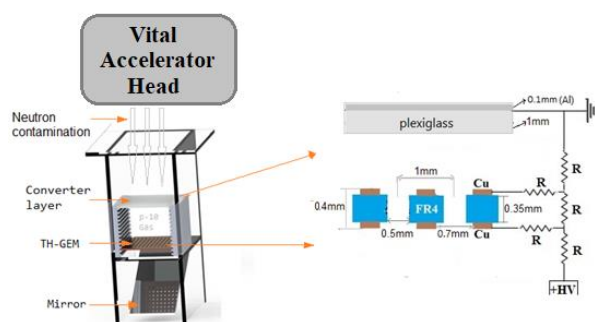


Figure 3. Schematic of the neutron detection system

According to Figure 3 the neutron contamination in collision with neutron-to-proton converter layer, produces accelerated protons. Neutron-to-proton converters can be made of materials containing Hydrogen compounds, such as plastic, CR-39 (Columbia Resin 1939), or Plexiglas. When neutrons

collide elastically with converter elements, their Hydrogen bonds are separated and accelerated protons are produced.

The accelerated protons proceed to ionize noble gas atoms in the vicinity of THGEM holes, generating secondary electrons within this sensitive region (Sensitive region: The cube enclosing the THGEM hole). By applying the appropriate voltage, the THGEM holes can be set in the Self-Quenching Streamer (SQS) mode, resulting in the creation of a spark or streamer. The intensity of these streamers depends on the secondary electrons density (Caused by ionization) and applied voltage to the detector. These streamers can be recorded with a camera during the detection period [35-37]. The number of streamers in THGEM, represents the amount of neutron contamination in treatment room.

Application of MCNPX code in the design of detection system

In this study, Monte Carlo N Particle-version X (MCNPX) is used for calculations. The MCNPX code is a simulation code based on Monte Carlo calculation methods, capable of tracking 32 nuclear and atomic particles [39]. There are three main components in input file: cell, surface, and data cards. The geometry of the detection system is designed using the surface and cell cards, while the data card includes items essential for dosimetry calculations and problem-solving. Key data card items involve defining the source, material, and the percentage composition of elements in the material. In this section, the effectiveness of the detection system presented in Figure 3 was evaluated through the MCNPX simulation code.

Neutron contamination energy spectrum: In the first step, the neutron contamination energy spectrum produced by the VITAL model of VARIAN LINAC is required. In this accelerator when high-energy electrons hit a target, they emit high-energy X-rays or gamma rays. The produced gamma rays cause the production of neutrons while they pass through the accelerator components, by (γ, n) interaction. Some examples of photo-neutron interactions with accelerator components are given as $^{184}\text{W}(\gamma, n)^{183}\text{W}$, $^{130}\text{Ba}(\gamma, n)^{129}\text{Ba}$, $^{89}\text{Br}(\gamma, n)^{88}\text{Br}$, $^{23}\text{Na}(\gamma, n)^{22}\text{Na}$, etc. Also, there is another possibility of interaction between the produced neutrons (Secondary neutrons), and the components of accelerator, by the (n, p) , (n, np) , (n, a) , (n, pa) , (n, n) , $(n, 2n)$, $(n, 3n)$, etc. interactions. Some examples of Secondary neutrons interactions with accelerator components are given as $^{184}\text{W}(n, 2n)^{183}\text{W}$, $^{130}\text{Ba}(n, 2n)^{129}\text{Ba}$, $^{89}\text{Br}(n, 2n)^{88}\text{Br}$, $^{23}\text{Na}(n, 2n)^{22}\text{Na}$, etc. that a is for alpha, pa is for proton and alpha, and np is for neutron and proton production. Moreover, the spallation process with gamma and neutron particles could happen. The presence of diverse elements in the linac head, such as Br, Ba, etc., enables photon and neutron reactions. In the photon or neutron spallation process with linac elements, a range of particles with mass numbers lower than the target mass number are produced. The probability of producing each of these particles depends

on the energy of primary particle. Probability of the earlier mentioned reactions in VARIAN LINAC, could be expressed using the cross-sectional area meaning. These calculations were done in a research and neutron contamination spectrum for 15 MeV electron beam energy of VITAL model of VARIAN LINAC has been obtained [40]. This energy spectrum was obtained at a distance of one meter from the LINAC head, i.e. at the location of the patient's bed. (Figure 4).

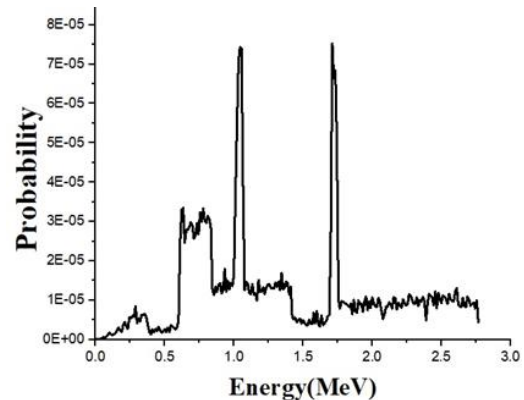


Figure 4. The energy spectrum of neutron contamination from VITAL model of VARIAN LINAC (SSD=1m) [40]

Proton production: The detection system is placed on the treatment bed so that the converter layer is one meter away from the accelerator head (SSD=1 m). In this situation, the energy spectrum of figure 4 was considered as the neutron source and the 1 mm thick Plexiglas converter layer as the target. When neutrons collide elastically with converter elements, their Hydrogen bonds are separated and protons are produced. The transferring energy (E) to mass number (A), is obtained as equation 1 [38].

$$E = [4A / (1+A)^2] [\text{Cos}^2 \theta] E_n \quad (1)$$

In the equation, E_n is the neutron energy and θ is the scattering angle of neutrons after hitting the target. This equation states that protons receive the most energy when they are produced by direct impact of neutrons with the target ($\theta=0$). In this step, the energy spectrum of the produced protons was determined using Tally F_2 .

Deposited energy of proton in gas: In fact, the absorbed energy by the detector gas (deposited energy of protons) is the ionization energy of the gas particles. In the simulation code, the energy spectrum of protons obtained from the converter was considered as a source and gas elements as targets. P-10 is the noble gas used in these calculations, this gas consists of a combination of 90% argon and 10% methane. The mesh tally card types 1 PEDEP command, has been used to extract deposited energy data in the active volume of the gas detector. By performing calculations, the maximum energy deposited (MeV/cm^3) in the gas elements at a certain distance from the converter was obtained. This distance is the best place to put THGEM.

THGEM applied voltage to achieve SQS mode: For THGEM holes to achieve SQS mode, the necessary

conditions must be met. 1- Filling the detector space with P-10 gas 2- Placing THGEM at a suitable distance from the converter, where the most energy of protons is deposited in gas elements 3- Rather condition. The first two conditions were examined in the previous sections. In this part, the third condition is examined. Khezripour et al found the function of voltage applied (V(v)) to the THGEM versus the remain energy in the sensitive region (E(MeV)) of the THGEM, by studying Rather condition in the THGEM detector. It is expressed by Equation 2 [41].

$$V = (0.2 - \log E) / 0.999 \tag{2}$$

If the voltage applied to the THGEM is sufficient, a single ion can create a streamer in one of the THGEM holes. All the results of MCNPX code calculations are given in the results section.

Results

In this section, the results of the MCNPX simulation code for the design of neutron contamination detection of VARIAN LINAC are presented. The results have shown that a Plexiglas layer with a thickness of 1 mm has an acceptable performance as a converter. Collision the neutron contamination of VITAL LINAC with this Plexiglas layer causes the product of accelerated protons. These protons can be absorbed by P-10 gas particles and ionize some of them. The absorbed energy by P-10 gas (deposited energy in P-10 gas) was obtained at various distances below the converter. The amount of energy deposited in the P-10 gas, as a function of the distance to the converter, is shown in Figure 5.

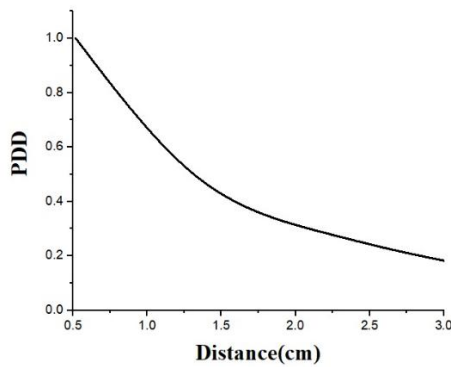


Figure 5. Relationship deposited energy in P- 10 gas as a function of distance to the converter

According to Figure 5, at distances closer to the converter, more energy is deposited in the gas elements. In other words, accelerated protons ionize more gas particles at closer distances to the converter. Of course, the best location for THGEM is the place where the most energy is deposited in the gas atoms. According to this result, a distance of 0.5 cm from the converter layer is a best position to place the THGEM. In Figure 6, the amount of deposited energy in P-10 gas elements is shown at a distance of 0.5 cm from the converter layer.

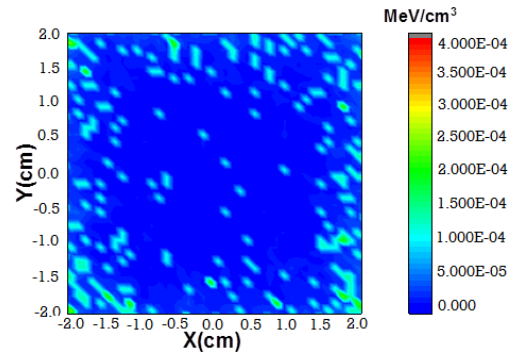


Figure 6. Deposited energy in P-10 gas by accelerated protons at the different locations of the THGEM

Considering the deposited energy in the sensitive region (Fig. 6), the voltage required to reach the SQS mode in THGEM holes was calculated using Equation 2. These results are shown in Figure 7.

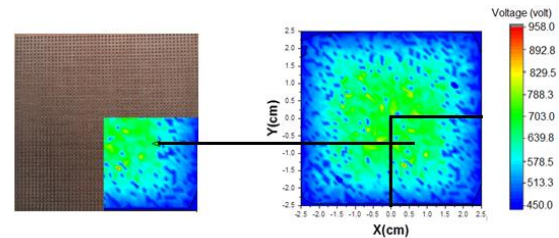


Figure 7. Voltage distribution to achieve SQS mode in the THGEM

According to Figure 7, by placing the results of these calculations on the THGEM board, the number of holes achieved the SQS mode in different voltage ranges is obtained. The relationship between voltage and number of holes that achieved to SQS mode is shown in Figure 8.

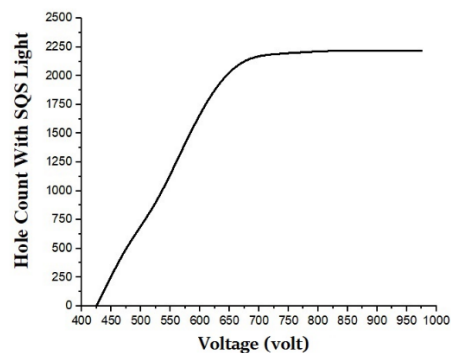


Figure 8. The plot of the number of holes that achieved to SQS mode and applied voltage to THGEM

According to Figure 8, when the voltage reaches 430 V, the THGEM holes are at the threshold of the SQS mode. At this moment a single ion can create a lighting (streamer) in one of THGEM holes. In the range between 430 and 700 volts, the number of streamers is proportional to the voltage. In other words, in this range, with increasing voltage, more holes of THGEM are placed in SQS mode. Streamer is occurring in almost every hole of the THGEM when the minimum voltage of it is 700 volts. In this case,

about 2150 holes of THGEM are placed in SQS mode. In general, the simulation results show that: neutron contamination for 15 MeV electron beam energy of VARIAN LINAC at SSD=1m, can create 2150 streamers in THGEM holes.

These streamers can be recorded by the camera at regular intervals. In fact, streamers of THGEM holes could represent the effect of neutron contamination on the converting layer. In other words, the number of streamers is a scale of the neutron contamination in the treatment room.

Discussion

In this research was tried to investigate the efficiency of THGEM in SQS mode to detect neutron contamination of medical linear accelerators by the simulation method. The simulation calculations (MCNPX code calculations) have confirmed the effectiveness of the proposed detection system for measuring Neutron contamination of VARIAN LINAC. Some of the most important results are: 1- The best distance between the converter and THGEM 2- The applied voltage in the best efficiency of the detection system 3- Number of THGEM holes in SQS mode (Number of streamers), caused by neutron contamination for 15 MeV VARIAN LINAC beam energy at SSD=1m. To reach clear achievement using THGEM for neutron detection, a part of the study results can improve the results of pervious research. In this study, the detection system of Figure 3 was built and the results were analyzed by using the Am-Be neutron source at a distance of 2 cm above the

converter. These results were compared with the results of a recent study.

Using the data in Table 1, the detection system was designed at the highest THGEM efficiency for the Am-Be neutron source. Some of the SQS modes in the THGEM holes recorded by the camera in this research are shown in Figure 9.

According to these results, 903 THGEM holes were in SQS mode, by using the Am-Be neutron source with 5 Ci activity at a distance of 2 cm from the converter layer; which was in agreement with MCNP code calculations. Moreover, the activity of this neutron source in THGEM holes was recorded at the rate of 31 SQS/s (THGEM activity in detecting neutron flux of Am-Be source \approx 31 SQS/s). The Am-Be neutron source with 5 Ci activity produces a neutron flux of about 1.1×10^7 n/s [42]. Therefore, the neutron flux at the location of the converting layer is about 2.2×10^5 n/cm²s. Based on the conducted studies, the maximum dose of linear accelerators with 15 MeV energy in SSD=1 m is about 1000 MU/min [43] and in another research conducted with this energy, the total neutron contamination through the head of accelerator has been obtained 2.8×10^6 n/cm²/Gy [44]. Therefore, the neutron contamination flux in SSD=1 m is estimated at 4.7×10^5 n/cm²s. Using these data and the data available in the results section, it is possible to compare both neutron sources (Am-Be neutron source with 5 Ci activity and Neutron contamination of VARIAN LINAC) in detection by THGEM (Table 2).

Table 1. THGEM structure in SQS mode at the best efficiency for detecting neutron contamination of VARIAN LINAC in comparison with detecting Am-Be neutron source

Neutron source	Source-Converter distance (cm)	converter-THGEM distance (cm)	Voltage applied to THGEM (volt)
Am-Be neutron source with 5 Ci activity	2	3	1020
Neutron contamination of VARIAN LINAC	100	0.5	700



Figure 9. some SQS modes created in the THGEM holes during the process of detecting neutrons from the AM-Be source

Table 2. THGEM output in the detection of neutron contamination of VARIAN LINAC compared to the detecting neutron of the Am-Be source

Neutron source	flux at the converter site (n/cm ² .s)	Number of THGEM holes in SQS mode	Percentage of THGEM holes in SQS mode (%)
Am-Be neutron source with 5 Ci activity	2.2x10 ⁵	903	34
Neutron contamination of VARIAN LINAC	4.7 x10 ⁵	2150	82

Results showed that the number of streamers have a direct relationship with neutron contamination. For this purpose, the detection system proposed in this study was practically tested with the Am-Be neutron source. Based on Table 2 results, the ratio of the VIRIAN LANIC neutron flux to the Am-Be neutron flux ($(4.7 \times 10^5) / (2.2 \times 10^5) = 2.14$) is in acceptable agreement with the ratio of the number of SQS holes created by these neutron sources ($(2150/903) = 2.38$). Therefore, the accuracy of THGEM detection system in SQS mode is acceptable and the simulation results in this study can be confirmed to estimate Neutron contamination using the proposed detection system. Results show in detecting the neutron flux of VARIAN LINIC, THGEM activity is 60 SQS/s that is twice the value obtained from the Am-Be neutron source flux THGEM activity.

Conclusion

The most important challenge of detecting neutron contamination in medical LINAC is neutron neutrality. In this study, by using THGEM in SQS mode, a new idea to detect neutron contamination was investigated. This method proposes simple systems of neutron contamination detection because this method requires less electrical circuits, compared to other neutron detectors. Also placing THGEM in SQS mode introduces small structures of neutron detectors. The main part of the detection system proposed in this study is the gap between the THGEM and the converter. According to the results, the highest efficiency of the detector is at short distances between the converter and THGEM (about 0.5 cm). Therefore, the volume of the detection system is acceptable for detecting the neutron contamination of LINAC. On the other hand, by considering the structure and price of THGEM, this system could be used in a larger detection area. Due to the short distance between the converter and the THGEM, the Streamer generated in the THGEM holes can determine the approximate location of proton production in the converter. In other words, the location of the holes in the SQS mode shows the approximate location of the neutron collision with the converter. Therefore, this study can suggest a suitable approach in location of neutron contamination. To achieve this goal, further research on this detection system in larger dimensions is needed.

Acknowledgment

The authors are very much thankful to Dr. Saeedeh Khezripour (Faculty of Sciences and Modern Technologies, Graduate University of Advanced Technology, Kerman, Iran) as she introduced the THGEM plate making company in Shiraz Province.

References

1. Mayles P, Nahum A, Rosenwald J-C. Handbook of radiotherapy physics: theory and practice: CRC Press. 2007.
2. Pena J, Franco L, Gomez F, Iglesias A, Pardo J, Pombar M. Monte Carlo study of Siemens PRIMUS photoneutron production. Phys Med Biol. 2005;50 (24):5921–33
3. Vega-Carrillo HR, Hernandez-Almaraz B, Hernandez-Davila VM, Ortiz-Hernandez. A Neutron spectrum and doses in a 18 MV LINAC. J Radioanal Nucl Chem. 2010;283(1):261–5.
4. Chadwick MB, Oblozinsky P, Blokhin A, Fukahori T, Han Y, Lee YO, et al. Handbook on photonuclear data for applications: cross sections and spectra. IAEA TECH-DOC 1178. 2000.
5. Garnica-Garza HM. Characteristics of the photoneutron contamination present in a high-energy radiotherapy treatment room. Phys Med Biol. 2005;50 (3):531–9.
6. Martinez-Ovalle SA, Barquero R, Gomez-Ros JM, Lallena AM. Ambient neutron dose equivalent outside concrete vault. rooms for 15 and 18 MV radiotherapy accelerators. Radiat Prot Dosim. 2012;148(4):457–64.
7. Carinou E, Stamatelatos IE, Kamenopoulou V, Georgolopoulou P, Sandilos P. An MCNP-based model for the evaluation of the photoneutron dose in high energy medical electron accelerators. Phys Med. 2005;21(3):95–9.
8. Saeed MK, Moustafa O, Yasin OA, Tuniz C, Habbani FI. Doses to patients from photoneutrons emitted in a medical linear accelerator. Radiat Prot Dosim. 2009;133(3):130–5.
9. Vega-Carrillo HR, Martinez-Ovalle SA, Lallena AM, Mercado GA, Benites-Rengifo JL. Neutron and photon spectra in LINACs. Appl Radiat Isot. 2012;71:75–80.
10. Ongaro C, Zanini A, Nastasi U, Rodenas J, Ottaviano G, Manfredotti C. Analysis of photoneutron spectra produced in medical accelerators. Phys Med Biol. 2000;45(12):55–61.
11. Lin JP, Liu WC, Lin CC. Investigation of photoneutron dose equivalent from high-energy photons in radiotherapy. Appl Radiat Isot. 2007;65(5):599–604.
12. Hsu FY, Chang YL, Liu MT, Huang SS, Yu CC. Dose estimation of the neutrons induced by the high energy medical linear accelerator using dual-TLD chips. Radiat Meas. 2010;45(3-6):739–41.
13. Mukherjee B, Makowski D, Simrock S. Dosimetry of highenergy electron linac produced photoneutrons and the bremsstrahlung gamma-rays using TLD-500

- and TLD-700 dosimeter pairs. *Nucl Instrum Methods Phys Res A*. 2005;545(3):830–41.
14. Alem-Bezoubiri A, Bezoubiri F, Badreddine A, Mazrou H, Lounis-Mokrani Z. Monte Carlo estimation of photoneutrons spectra and dose equivalent around an 18MV medical linear accelerator. *Radiat Phys Chem*. 2014;97:381–92.
 15. Al-Ghamdi H, Al-Jarallah MI, Maalej N. Photoneutron intensity variation with field size around radiotherapy linear accelerator 18-MeV X-ray beam. *Radiat Meas*. 2008;43:S495–9.
 16. Barquero R, Mendez R, Vega-Carrillo HR, Iniguez MP, Edwards TM. Neutron spectra and dosimetric features around an 18 MV linac accelerator. *Health Phys*. 2005;88(1):48–58.
 17. Domingo C, Garcia-Fuste MJ, Morales E, Amgarou K, Terron JA, Rosello J, et al. Neutron spectrometry and determination of neutron ambient dose equivalents in different LINAC radiotherapy rooms. *Radiat Meas*. 2010;45(10):1391–7.
 18. Barros S, Mares V, Bedogni R, Reginatto M, Esposito A, Goncalves IF, et al. Comparison of unfolding codes for neutron spectrometry with Bonner spheres. *Radiat Prot Dosim*. 2014;161(1-4):46–52.
 19. Garny S, Mares V, Roos H, Wagner FM, Ruhm W. Measurement of neutron spectra and neutron doses at the Munich FRM II therapy beam with Bonner spheres. *Radiat Meas*. 2011;46(1):92–7.
 20. Howell RM, Kry SF, Burgett E, Hertel NE, Followill DS. Secondary neutron spectra from modern Varian, Siemens, and Elekta linacs with multileaf collimators. *Med Phys*. 2009;36(9):4027–38.
 21. Vega-Carrillo HR, Ortiz-Hernandez A, Hernandez-Davila VM, Hernandez-Almaraz B, Montalvo TR. H*(10) and neutron spectra around linacs. *J Radioanal Nucl Chem*. 2010;283(2):537–40.
 22. Banaee N, Goodarzi K, Nedaie H A. Neutron contamination in radiotherapy processes: a review study. *Journal of Radiation Research*. 2021;62(6):947-54.
 23. Tai DT, Loan TT, Sulieman A, Tamam N, Omer H, Bradley DA. Measurement of Neutron Dose Equivalent within and Outside of a LINAC Treatment Vault Using a Neutron Survey Meter. *Quantum Beam Science*. 2021;5(4):33.
 24. Elmtalab S, Abedi I, Alirezaei Z, Choopan Dastjerdi MH, Geraily G, Karimi AH. Semi-experimental assessment of neutron equivalent dose and secondary cancer risk for off-field organs in glioma patients undergoing 18-MV radiotherapy. *Plos one*. 2022;17(7):e0271028.
 25. Sohrabi M, Torkamani ME. Breakthrough whole body energy-specific and tissue-specific photoneutron dosimetry by novel miniature neutron dosimeter/spectrometer. *Scientific Reports*. 2021;11(1):20552.
 26. Pietropaolo A, Claps G, Fedrigo A, Grazzi F, Höglund C, Murtas F, et al. Neutron diffraction measurements on a reference metallic sample with a high-efficiency GEM side-on 10B-based thermal neutron detector. *EPL (Europhysics Letters)*. 2018;121(6): 62001.
 27. Santoni A, Celentano G, Claps G, Fedrigo A, Höglund C, Murtas F, et al. Physical–chemical characterization of a GEM side-on 10B-based thermal neutron detector and analysis of its neutron diffraction performances. *Nuclear Instruments and Methods in Physics Research Section A: Accelerators, Spectrometers, Detectors and Associated Equipment*. 2018;906:83-7.
 28. Song D, Choi K, Jeng Y, Kang Y, Lee J S H, Park I, et al. Neutron Detection using a Gadolinium-Cathode GEM Detector. *arXiv preprint arXiv:2012.2020:02546*.
 29. Zhou J, Zhou J, Zhou X, Zhu L, Wei Y, Xu H, et al. A sealed ceramic GEM-based neutron detector. *Nuclear Instruments and Methods in Physics Research Section A: Accelerators, Spectrometers, Detectors and Associated Equipment*. 2021;995:165129.
 30. Ohshita H, Uno S, Otomo T, Koike T, Murakami T, Satoh S, et al. Development of a neutron detector with a GEM. *Nuclear Instruments and Methods in Physics Research Section A: Accelerators, Spectrometers, Detectors and Associated Equipment*. 2010;623(1): 126-8.
 31. Croci G, Claps G, Cavenago M, Dalla Palma M, Grosso G, Murtas F, et al. nGEM fast neutron detectors for beam diagnostics. *Nuclear Instruments and Methods in Physics Research Section A: Accelerators, Spectrometers, Detectors and Associated Equipment*. 2013;720: 144-8.
 32. Zhou J, Zhou X, Zhou J, Jiang X, Yang J, Zhu L, et al. A novel ceramic GEM used for neutron detection. *Nuclear Engineering and Technology*. 2020;52(6):1277-81.
 33. Yang L, Zhou J-R, Sun Z-J, Zhang Y, Huang C-Q, Sun G-A, et al. Experimental research on a THGEM-based thermal neutron detector. *Chinese Physics C*. 2015;39(5): 056002.
 34. Anjomani Z, Hanu A, Prestwich W, Byun S. Monte Carlo design study for thick gas electron multiplier-based multi-element microdosimetric detector. *Nuclear Instruments and Methods in Physics Research Section A: Accelerators, Spectrometers, Detectors and Associated Equipment*. 2014;757: 67-74.
 35. Souiri R, Negarestani A, Mahani M. A new approach for direct imaging of Alpha radiation by using Micro Pattern Gas Detectors in SQS mode. *Nuclear Instruments and Methods in Physics Research Section A: Accelerators, Spectrometers, Detectors and Associated Equipment*. 2018;884: 128-35.
 36. Souiri R, Negarestani A, Mahani M. Alpha radiation detection by using of Micro Pattern Gas Detectors in SQS mode. *Iranian Journal of Radiation Safety and Measurement*. 2017; 5(2):29-38.
 37. Hashemi S M, Negarestani A. Investigation of alpha particle tracks in GEM-type structures based on SQS mode. *Nuclear Instruments and Methods in Physics Research Section A: Accelerators, Spectrometers, Detectors and Associated Equipment*. 2019;913: 20-7.
 38. Glenn E Knoll, *Radiation Detection and Measurement*. Third Edition. 2000; chapter 15, Page 554, ISBN 0-471-07338-5.
 39. Werner C J. *MCNP users-manual-code version 6.2*. Los Alamos national laboratory. 2017.

40. Zarei N, Rezaie M R, Jomehzadeh A. Neutron leakage Calculation of Varian accelerator in Kerman Radiotherapy and Oncology Center, National Conference on Technological Advances in Applied Physics, Kerman-Iran, March 2022.
41. Khezripour S, Negarestani A, Rezaie M. A New Approach for Alpha Radiography by Triple THGEM using Monte Carlo Simulation and Measurement. *Journal of Instrumentation*. 2018;13(05): P05024.
42. Kotba NA, Tohamyb MM, Soliemanb AHM, El-Zakla T, Amer TZ, Elmeniawi S, et al. Characterization of ^{241}Am -be neutron source using threshold foil activation technique. *Al-Azhar Bulletin of Science*. 2019; 30(1-B):48-53.
43. Schüller E, Trovati S, King G, Lartey F, Rafat M, Villegas M, et al. Experimental platform for ultra-high dose rate FLASH irradiation of small animals using a clinical linear accelerator. *International Journal of Radiation Oncology*Biophysics*. 2017;97(1):195-203.
44. Hill T M. Neutron Fluence Measurements of the Siemens Oncor Linear Accelerator Utilizing Gold Foil Activation. Medical University of Ohio. 2005.